



## Comparison of statistical methods to predict fouling propensity of microfiltration membranes for drinking water treatment

Jaehyun Ju, Youngkyu Park, Yongjun Choi, Sangho Lee\*

School of Civil and Environmental Engineering, Kookmin University, Jeongneung-Dong, Seongbuk-Gu, Seoul, 136-702, Republic of Korea, Tel. +82 2 910 4529; Fax +82 2 910 4939; email: sanghlee@kookmin.ac.kr (S. Lee)

Received 31 August 2018; Accepted 15 October 2018

### ABSTRACT

This paper investigated the feasibility and limitation of statistical models to predict membrane fouling in a pilot-scale system. Operation data from an MF pilot plant with the capacity of 440 m<sup>3</sup>/d were used for the application of these models. Water quality parameters including feed water turbidity, algae concentration, total organic carbon, dissolved organic carbon, and UV<sub>254</sub> absorbance were correlated with transmembrane pressure, total resistance, and the rate of resistance change. Model fit equations were derived from multiple linear regression, artificial neural network, genetic programming, and support vector machine. The performances of models were compared in terms of accuracy and prediction capability.

*Keywords:* Microfiltration; Fouling; Statistical analysis; Artificial neural network; Support vector machine; Genetic programming

### 1. Introduction

Microfiltration (MF) processes have been applied for drinking water treatment and wastewater reclamation because it has abilities to remove various particles, colloids, iron/manganese after oxidation and disinfection byproduct precursors [1–4]. Moreover, MF also allows a small footprint, reduced use of chemicals, and possibility of unmanned operation [2]. In addition, the MF can be used for the pretreatment of the feed water for reverse osmosis and nanofiltration processes [5,6]. This is because MF offers a higher removal efficiency of colloidal materials than conventional pretreatment technologies [6,7], resulting in a lower silt index (SDI) values.

However, MF generally suffers from a serious problem associated with membrane fouling [8,9]. Since membrane fouling is an inherent problem, it is not possible to completely avoid it [10–12]. Once it occurs, the membrane performance decreases, the operation cost increases, and the lifespan of the membrane is shortened [1,9,13–15]. Thus, it is desired to predict the progress of membrane fouling for predictive operation maintenance of MF processes [10,13,16].

Unfortunately, it is extremely difficult to accurately predict membrane fouling in large-scale MF processes because there are many factors that cannot be easily controlled, including feed water qualities and temperatures [17–20].

To overcome the limitations of fouling prediction methods, a handful of works have been done by applying various statistical models such as artificial neural network (ANN) [9,17,21–24]. Using these statistical models, accurate fitting to non-linear behaviors of membrane process in both small and large-scale systems is possible [17,22,25]. In addition, statistical models can identify key factors that affect membrane fouling and improve process operation and control reliability [22]. Nevertheless, relatively few works have been done to compare different statistical models for MF fouling prediction in pilot- or full-scale processes [18,20,23].

In light of this issue, the purpose of this study was to compare the performance of multiple linear regression model (MLRM), ANN, genetic programming (GP), and support vector machine (SVM) for predicting membrane fouling in an MF pilot plant using feed water qualities and operational parameters. The inherent limitations of such approaches

\* Corresponding author.

were also compared from this analysis. To the best knowledge of the authors, this is the first study to compare more than four statistical models for MF fouling prediction in a pilot-scale, which provides insight into the optimization of fouling prediction in commercial-scale membrane plants.

## 2. Materials and methods

### 2.1. Pilot plant conditions

The operational data were collected from an MF pilot plant, the schematic diagram of which is shown in Fig. 1. The feed water for the pilot plant was the surface water from Han river, Korea. It was treated by coagulation and sedimentation prior to MF. The membrane used in the pilot plant was a submerged MF membrane module (CMF-S) manufactured by the Evoqua Memcor. The plant could produce the treated water of 440 m<sup>3</sup>/d. It was operated in the constant flow mode with a flux of approximately 47 L/m<sup>2</sup> h. The pilot plant was operated for 224 d and pH, temperature, turbidity, algae count, TOC, DOC, UV<sub>254</sub> were monitored.

### 2.2. Statistical modeling approach

As previously mentioned, several modeling approaches were applied to predict MF fouling in the pilot plant. Four statistical models were used including MLRM, ANN, GP, and SVM. Since there was no program that is capable of implementing all the models, different software tools were used: The analysis based on MLRM was performed using Minitab. The ANN analysis was carried out using WEKA. The GP model fits and SVM regression were done by GPdotNET

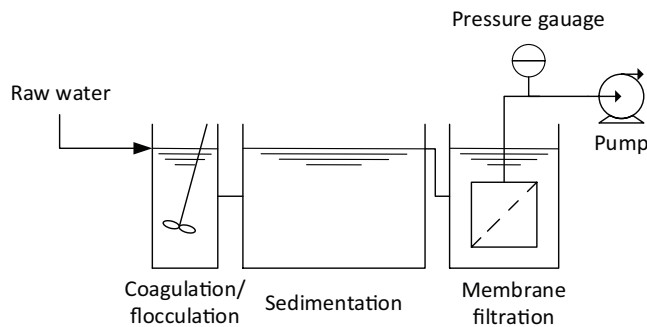


Fig. 1. Schematics of MF pilot plant for surface water treatment.

and MATLAB SVM Toolbox, respectively. Table 1 summarizes the definitions and programs for the statistical models. Each model requires different parameters and conditions for the analysis of the data. The appropriate modeling conditions were determined by trial and error methods, which are shown in Table 2. Although it is desired to use the same analysis tool for all the analysis, it could not be done due to the lack of the tool that can carry out all the analysis.

### 2.3. Hermia model

In addition to the statistical models, the Hermia model was also used to predict the MF pilot plant data [19,25]. Four blocking models including complete blocking (CB), standard blocking (SB), intermediate blocking (IB), cake filtration (CF) were considered for the constant flux operation. Table 3 summarizes the Hermia model equations, where  $p_0$  is the initial TMP,  $p$  is the TMP at time  $t$ ,  $J_0$  is the flux, and  $K_p$ ,  $K_s$ ,  $K_i$  and  $K_c$  are the model fit parameters for CB, SB, IB, and CF, respectively. Details on the Hermia model were previously reported [19].

Table 1  
Statistical model used to predict membrane fouling of pilot plant

Models	Definition	Program/platform
Multiple linear model	Fitting a linear equation to observed data with many variables	Minitab
ANN model	Simulation of the way in which the human brain processes information	WEKA [24]
GP model with simple functions	Derivation of (algebraic) equations to fit observed data	GPdotNET [26]
GP model with complex functions	Derivation of (nonlinear) equations to fit observed data	GPdotNET [26]
SVM regression	Use of discriminative classifier defined by a separating hyperplane to fit observed data	MATLAB SVM Toolbox

Table 2  
Statistical model parameters and options used to predict membrane fouling of pilot plant

Models	Conditions
Multiple linear model	Tolerance: 0.0001, confidence interval: 95%
ANN model	Learning rate: 0.3, momentum: 0.2, training time: 500, hidden layers: automatically determined
GP model with simple functions	Population size: 500, generation: 250, crossover: 0.9, mutation: 0.05, reproduction: 0.2, rank value: 0.8, operators: +, -, *, /
GP model with complex functions	Population size: 500, generation: 250, crossover: 0.9, mutation: 0.05, reproduction: 0.2, rank value: 0.8, operators: +, -, *, /, x <sup>2</sup> , x <sup>3</sup> , sin, cos, tan, exp, ln
SVM regression	SVM type: regression (epsilon SVR), kernel type: radial basis function, gamma: 0.125, C value: 1, epsilon value: 0.1

### 3. Results and discussions

#### 3.1. Water quality parameters

Water quality parameters for the feed water to the MF pilot plant were continuously monitored as shown in Fig. 2. The pilot plant began operation in winter and stopped in

summer. Thus, the temperature of the feed water increased with time. The maximum and minimum temperatures were 26.8°C and 1.574°C, respectively, and the average value was 16.285°C (Fig. 4(a)). The pH values ranged from 6.9 to 8.5. The maximum and minimum turbidities were 105.97 and 3.462 NTU, respectively, and the average value was 11.424 NTU (Fig. 4(b)). Near the end of the operation, the turbidity rapidly increased because the rainy season started. The algae counts were high in the beginning and became low after the operation of 80 d. The maximum and minimum UV<sub>254</sub> values were 0.085 and 0.014 cm<sup>-1</sup>, respectively, with the average value of 0.048 cm<sup>-1</sup> (Fig. 4(c)). TOC and DOC values decreased with time because they were generally high in winter seasons.

Table 3  
Hermia model equations for constant flux operation

Models	Equation
Complete blocking (CB),	$\frac{p_0}{p} = 1 - K_b J_0 t$
Standard blocking (SB)	$\left(\frac{p_0}{p}\right)^{0.5} = 1 - K_s J_0 t$
Intermediate blocking (IB)	$\ln\left(\frac{p}{p_0}\right) = K_i J_0 t$
Cake filtration (CF)	$\frac{p}{p_0} = 1 + K_c J_0 t$

#### 3.2. Pilot plant operation data and water quality parameters

Fig. 3 shows the operational data of the MF pilot plant. The changes in flux and transmembrane pressure (TMP) were shown as a function of the operation time. Since the plant was run at the constant flux mode, the flux did not significantly vary with time. The TMP increased with time due to the accumulation and deposition of foulants on the membrane. After 60 d, the TMP exceeded 60 kPa and thus the cleaning in place (CIP) of the membrane was carried out,

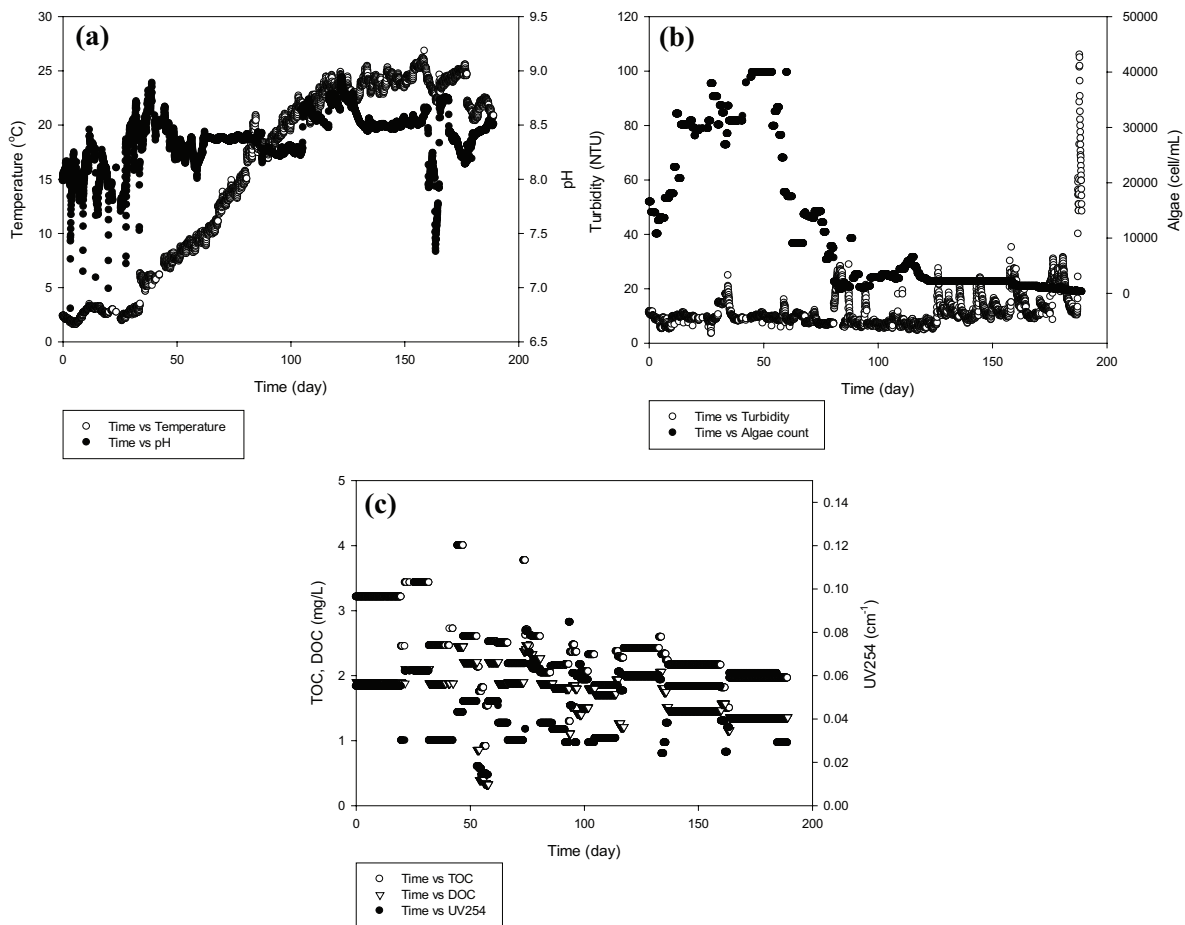


Fig. 2. Changes in water quality parameters with operation time: (a) feed temperature, pH; (b) water turbidity, algae count; and (c) TOC, DOC, and UV<sub>254</sub> absorbance.

resulting in the reduction in TMP from 64 kPa to 30 kPa. Then the plant was operated again during 164 d. Before the CIP, the pilot plant operation was carried out in the winter season with the feed water temperature less than 8°C. After the CIP, the pilot plant operation was mostly done in the spring and summer seasons. Considering the CIP event and the operational history of the pilot plant, the data analysis

was divided into 1st phase (winter) and 2nd phase (spring, summer) based on CIP.

3.3. Application of different methods

3.3.1. Hermia model

To begin, the Hermia models were applied to predict the TMP of the MF pilot plant. The results of the Hermia model application to the operation data in the 1st phase are shown in Fig. 4. The symbols indicate the experimental data and the lines indicate the model fits. As demonstrated in the plots, the Hermia models did not match the experimental data well. The  $R^2$  values for the complete blocking, standard blocking, intermediate blocking, and cake formation were only 0.587, 0.586, 0.568, and 0.505, respectively. Among these models, the complete blocking model showed the highest  $R^2$  value. Similar results were observed with the application of the Hermia models to the pilot data in the 2nd phase as shown in Fig. 5. In this case, the  $R^2$  values for the complete blocking, standard blocking, intermediate blocking, and cake formation were even lower, which were 0.194, 0.202, 0.213, and 0.226, respectively. Among these models, the cake formation model showed the highest  $R^2$  value.

Fig. 6 shows the predictions of TMP in the pilot plant using the Hermia models. The complete blocking model and cake formation model were used to fit the data in the 1st and 2nd phases, respectively. It is evident from the results that the Hermia models are not suitable to fit or predict the

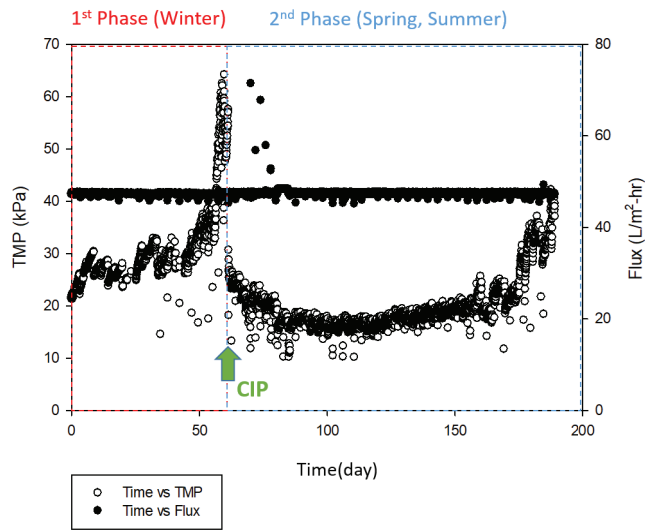


Fig. 3. Changes in flux and TMP with operation time.

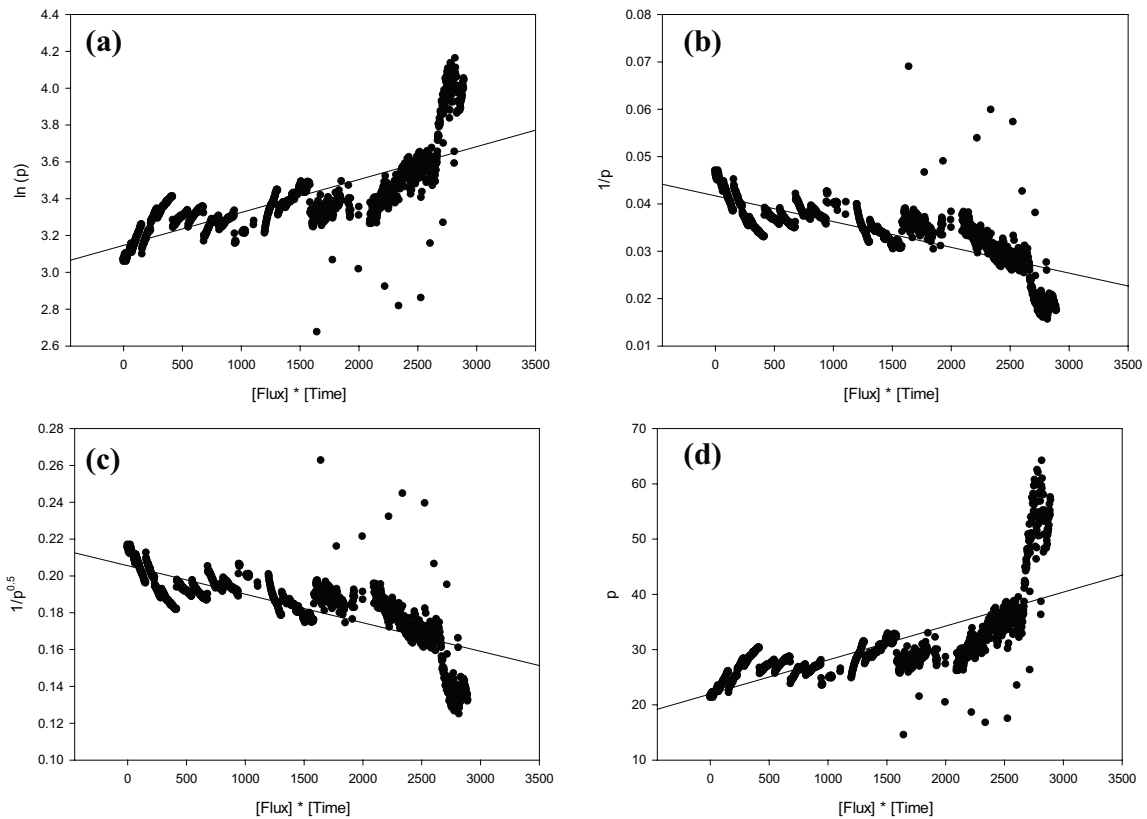


Fig. 4. Model fits to the operation data in the 1st phase (winter) using the Hermia’s model equations: (a) complete blocking, (b) standard blocking, (c) intermediate blocking, and (d) cake formation.

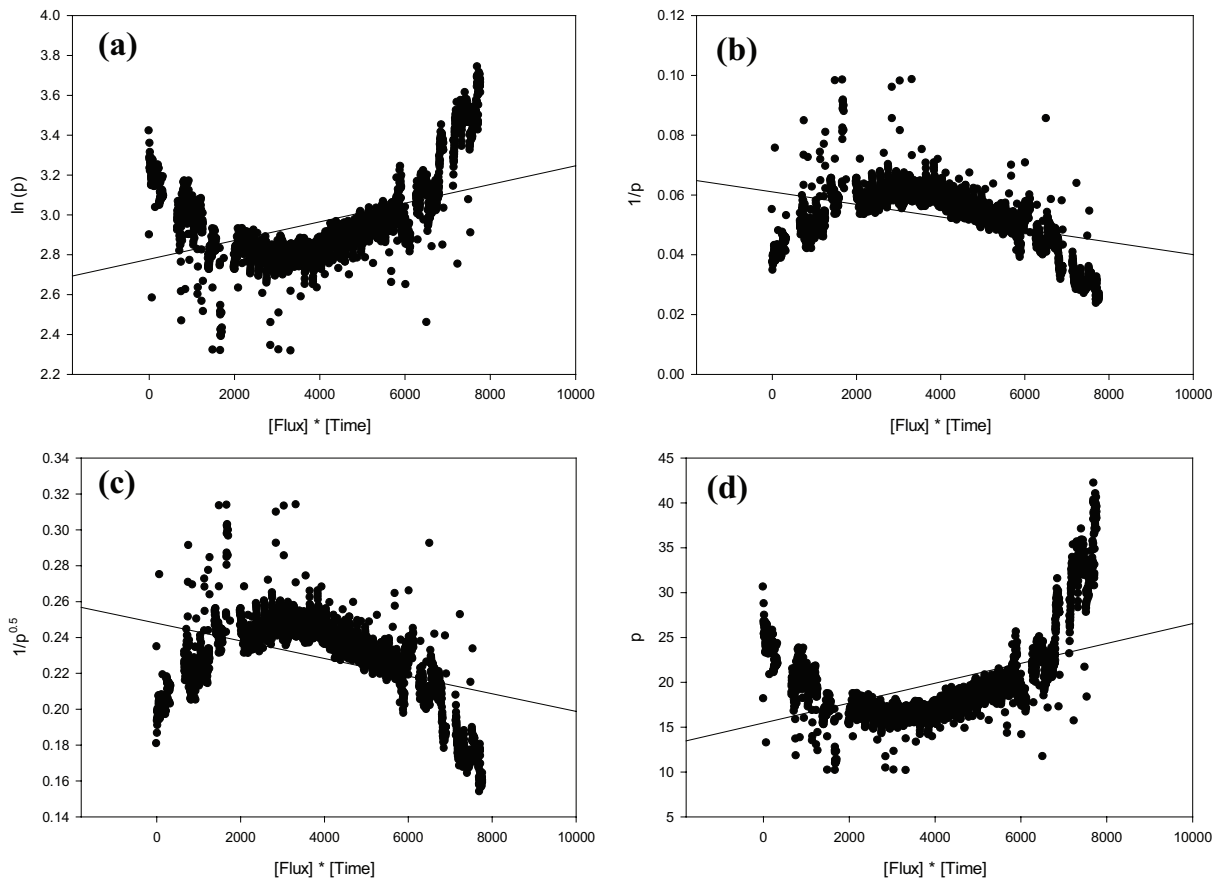


Fig. 5. Model fits to the operation data in the 2nd phase (spring and summer) using the Hermia’s model equations: (a) complete blocking, (b) standard blocking, (c) intermediate blocking, and (d) cake formation.

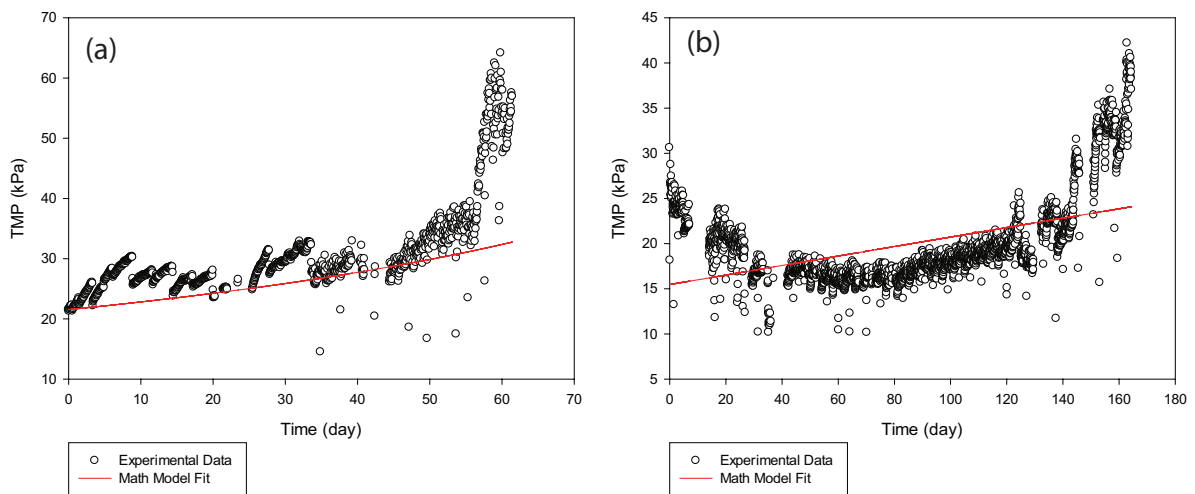


Fig. 6. Comparison of TMP of the pilot plant operation with the model predictions using the Hermia’s model equations: (a) 1st phase and (b) 2nd phase.

operation data in pilot plants. Since the TMP data in the pilot plant were highly non-linear, it is not possible to predict them using the simple mathematical models. Moreover, the Hermia models do not use water quality parameters as their independent variables and thus they cannot reflect the effect of water quality changes with time.

### 3.3.2. Multiple linear regression

Since the mathematical models based on the Hermia equations were not useful to predict the pilot data, statistical models were applied to obtain better model fits. Multiple linear regression (MLR) was applied as one of the statistical

models [18]. MLR allows to use several variables at once to explain the variation in a continuous dependent variable. It can isolate the unique effect of one variable on the continuous dependent variable while taking into consideration that other variables are affecting. The results of the model application are shown in Fig. 7. Compared with the Hermia model, the model predictions were much better, suggesting that MLR has potential for more accurate model predictions than the Hermia models. As a result of the model application, the MLR equations are given by:

$$P = -133.1 + 0.5655t - 1.405\text{pH} + 8.392 \times 10^{-02} c_{\text{turbidity}} - 0.2515T - 5.349 \times 10^{-04} c_{\text{algae}} - 1.633c_{\text{TOC}} - 1.952c_{\text{DOC}} + 252.2 C_{\text{UV254}} + 3.615 J \quad (1)$$

$$P = 8.720 + 0.1544t + 3.371\text{pH} + 0.1048c_{\text{turbidity}} - 1.503T - 3.259 \times 10^{-05} c_{\text{algae}} + 1.712c_{\text{TOC}} - 1.047c_{\text{DOC}} - 0.7692C_{\text{UV254}} - 4.799 \times 10^{-2} J \quad (2)$$

where  $P$  is the TMP (kPa);  $t$  is the operation time (d);  $c_{\text{turbidity}}$  is the feed water turbidity (NTU);  $T$  is the feed temperature ( $^{\circ}\text{C}$ );  $c_{\text{algae}}$  is the algae count of the feed water (cell/mL);  $c_{\text{TOC}}$  is the TOC of the feed water (mg/L);  $c_{\text{DOC}}$  is the DOC of the feed water (cell/mL); and  $J$  is the flux ( $\text{L}/\text{m}^2 \text{ h}$ ).

### 3.3.3. Artificial neural network

In addition to MLR, other statistical approaches were also applied. Fig. 8 shows the results of ANN application to the TMP data in the pilot plant. Similar to MLR, ANN showed good matches with the experimental data. However, it seems to be too sensitive to follow the experimental errors (overfitting) in some cases. For example, the TMP data between 34 d and 55 d in the 1st phase include several outliers and should not be considered in the model predictions. However, the ANN fitted these data points, leading to inappropriate model predictions. The overfitting may be

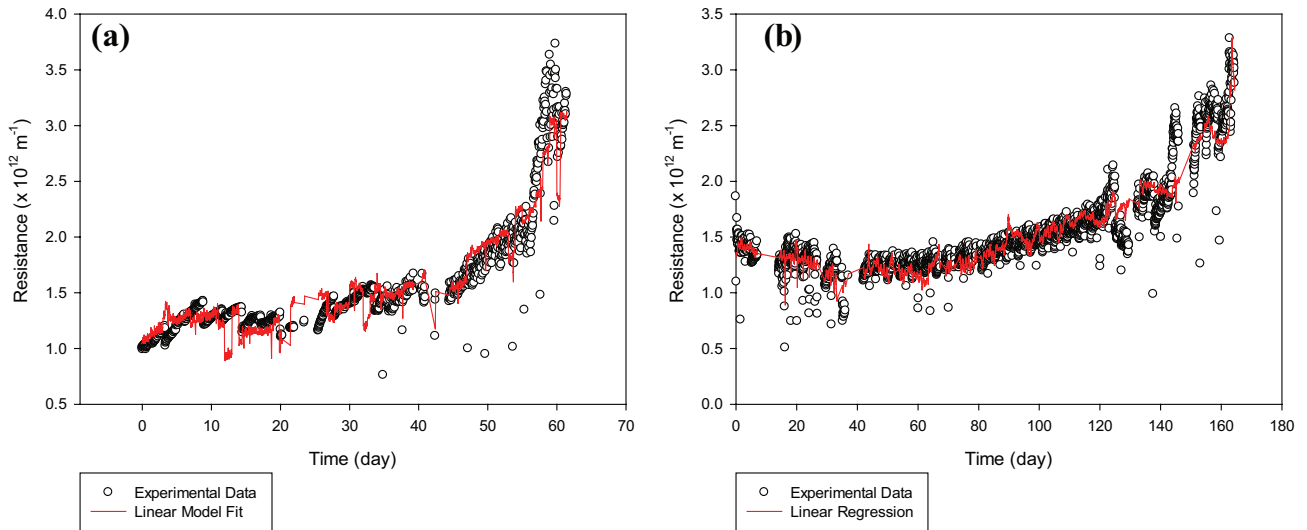


Fig. 7. Comparison of TMP of the pilot plant operation with the model predictions using MLR: (a) 1st phase and (b) 2nd phase.

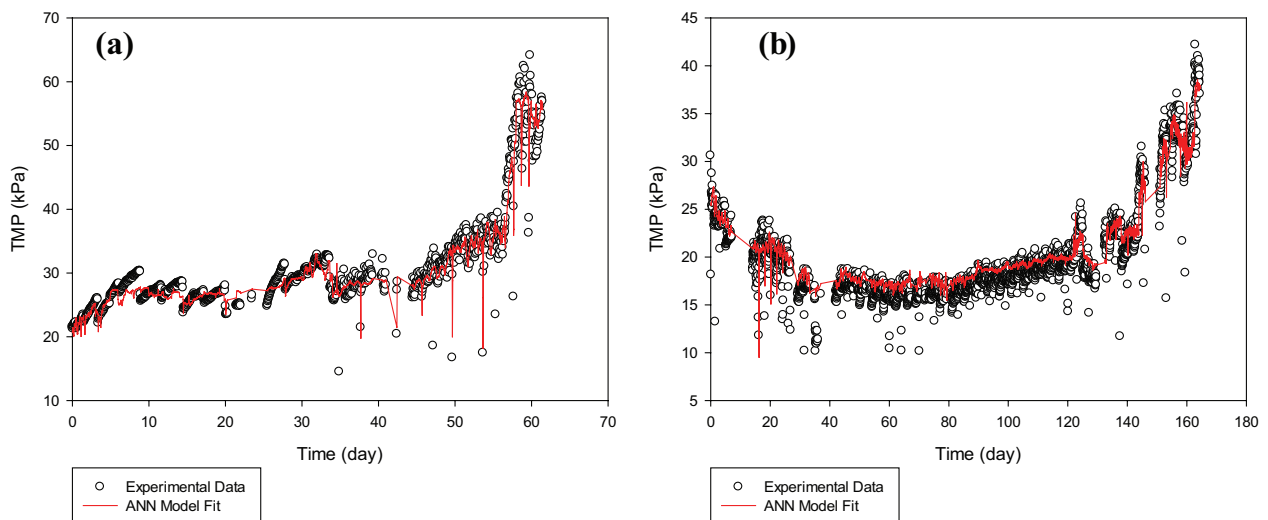


Fig. 8. Comparison of TMP of the pilot plant operation with the model predictions using ANN: (a) 1st phase and (b) 2nd phase.

avoided by adjusting the ANN model parameters. However, with the current model predictions, the overfitting seems to be an issue.

### 3.3.4. Statistical model: genetic programming

GP offers a solution through the evolution of computer programs by methods of natural selection [23,25]. GP searches the space of possible computer programs for a program that is highly fit for solving the problem at hand. Accordingly, GP offers a design method that automatically generates design solutions for multi-domain dynamic systems.

Two different approaches were attempted for the application of GP to model the MF pilot data. First, only simple algebraic operators such as '+', '-', '\*', and '/' were used to develop the model equation. Then, not only the simple operators but also complex functions such as 'sin', 'cos', 'tan', 'exp', 'ln', 'x<sup>2</sup>', and 'x<sup>3</sup>' were used to develop the model equations. The results are shown in Fig. 9 (simple operators) and Fig. 10 (complex functions). The GP based on simple operators shows reasonable fits to the plant data and is less sensitive to experimental errors and data hunting. Since the

noise from the data set was removed, the data smoothing was done by the GP model based on the simple operators. On the other hand, the GP based on complex functions provided the model fit that is less accurate than that by the GP based on simple operators. This implies that the selection of complex functions may not be helpful to improve the model prediction.

### 3.3.5. Statistical model: support vector machine regression

Support vector machine (SVM) regressions are used for the classification of tasks ranging from text to genomic data [27]. SVMs can be applied to complex data types beyond feature vectors by designing kernel functions for such data. SVM techniques have been extended to a number of tasks such as regression, principal component analysis, etc. Fig. 11 shows the model prediction by SVM for the MF pilot operation data. Overall, SVM matches the experimental data well. Unlike ANN, overfitting was not serious for SVM. But the application of SVM may be limited just similar to ANN because the final model is not expressed as a form of mathematical functions.

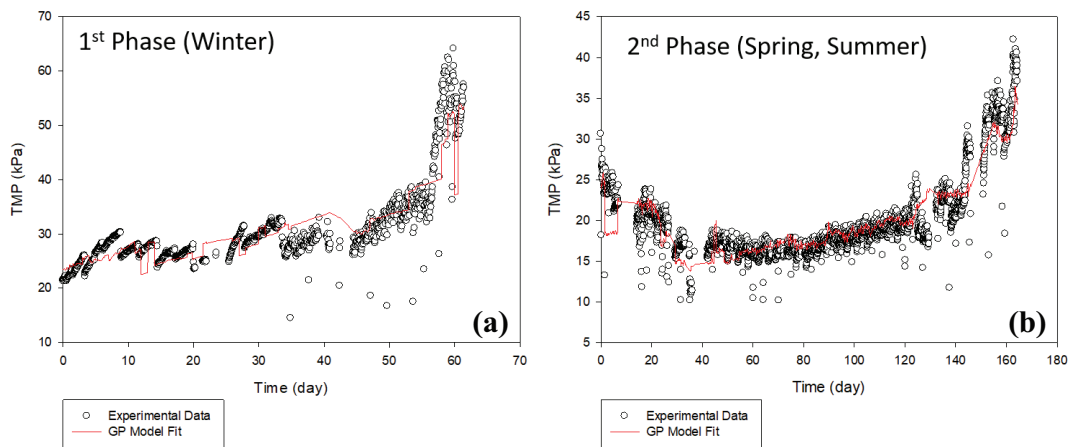


Fig. 9. Comparison of TMP of the pilot plant operation with the model predictions using GP based on simple operators: (a) 1st phase and (b) 2nd phase.

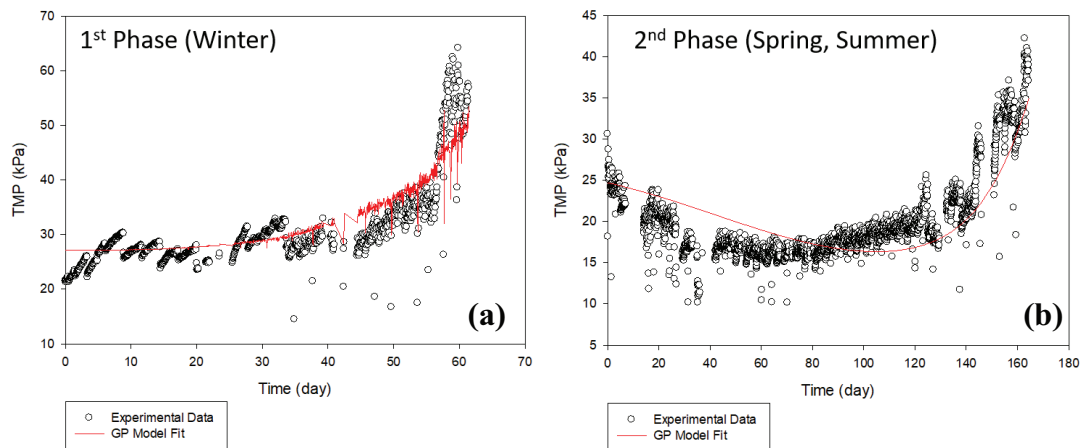


Fig. 10. Comparison of TMP of the pilot plant operation with the model predictions using GP based on complex functions: (a) 1st phase and (b) 2nd phase.

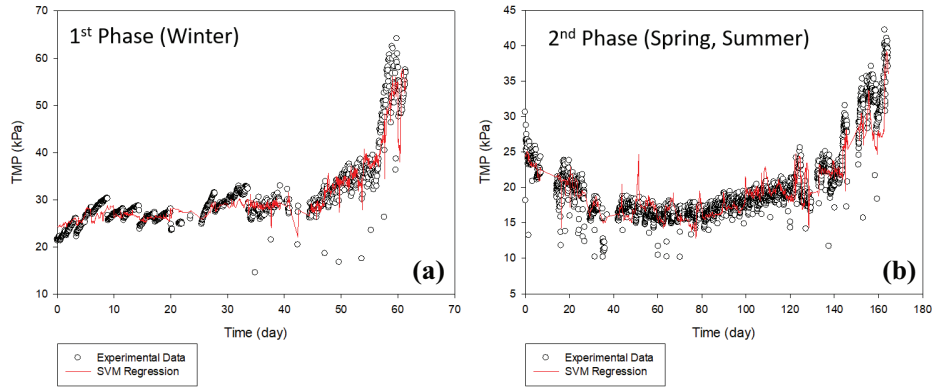


Fig. 11. Comparison of TMP of the pilot plant operation with the model predictions using SVM: (a) 1st phase and (b) 2nd phase.

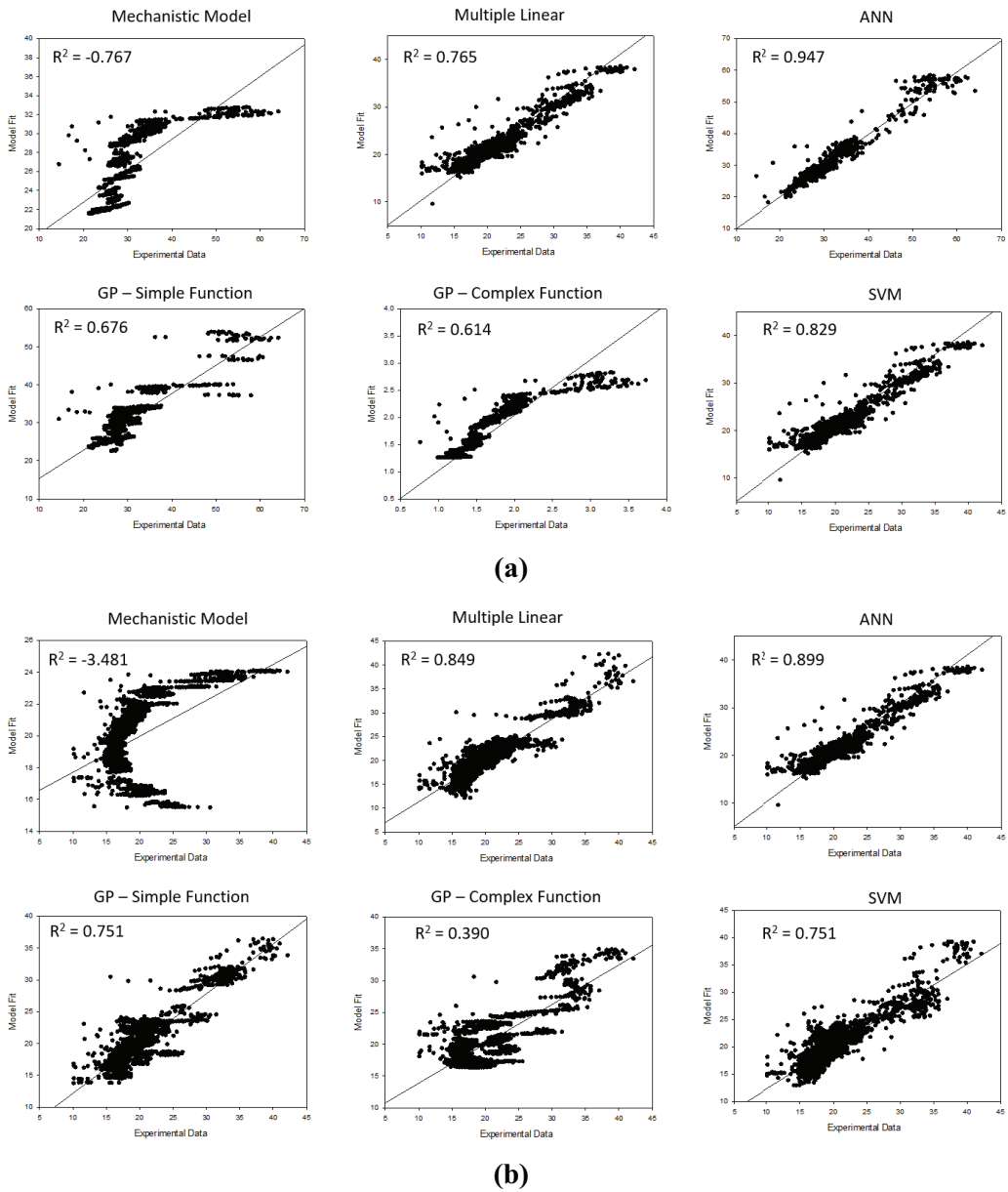


Fig. 12. Comparison of model predictions with MF pilot plant data: (a) 1st phase and (b) 2nd phase.

### 3.4. Comparison of different methods

The results of model predictions by different approaches were compared with the MF pilot plant data as shown in Fig. 12. The  $R^2$  in each case was also shown in the plot. As previously mentioned, mechanistic model based on the Hermia equation did not provide reasonable model predictions. On the other hand, the statistical models resulted in good agreements with the plant data. Among them, the ANN showed the highest  $R^2$  values (0.947 and 0.899) but suffered from the problem of overfitting. MLR and SVM also matched the data well. The  $R^2$  values for MLR were 0.765 for the 1st phase and 0.849 for the 2nd phase. The  $R^2$  values for SVM were 0.829 for the 1st phase and 0.751 for the 2nd phase. The GP based on simple operators showed lower  $R^2$  values (0.676 and 0.751) than ANN, MLR, and SVM but it can smooth the data. The GP based on complex functions showed the similar prediction performance to the GP based on simple operators.

### 4. Conclusions

In this study, the fouling behaviors of MF membranes in a pilot plant for surface water treatment were analyzed using statistical models. The following conclusions were withdrawn:

- Mechanistic models based on Hermia equations failed to fit the operation data in the MF pilot plant.
- Among the models considered in this study, ANN showed the highest  $R^2$  values. However, it is not easy to use ANN for the plant operation because the final model is not expressed as a form of mathematical functions. Overfitting to experimental errors and data hunting is also problematic.
- Multiple linear regression seems to be appropriate because it showed reasonably high  $R^2$  values and simple equations can be obtained.
- SVM regression was nearly as good as the MLR. But it has same limitations as ANN because the final model is not expressed as a form of mathematical functions.
- GP models have advantages over ANN and SVM because the models can be obtained as forms of simple function. However, the  $R^2$  values were not as high as those from MLR, ANN, or SVM.

### Acknowledgments

This work is supported by the Korea Agency for Infrastructure Technology Advancement (KAIA) grant funded by the Ministry of Land, Infrastructure and Transport (Grant 18FIP-B116951-03) and by Korea Ministry of Environment as “Global Top Project (2017002100001)”.

### References

- [1] J. Meier-Haack, N.A. Booker, T. Carroll, A permeability-controlled microfiltration membrane for reduced fouling in drinking water treatment, *Water Res.*, 37 (2003) 585–588.
- [2] A. Bottino, C. Capannelli, A. Del Borghi, M. Colombino, O. Conio, Water treatment for drinking purpose: ceramic microfiltration application, *Desalination*, 141 (2001) 75–79.
- [3] C. Teodosiu, A.-F. Gilca, G. Barjoveanu, S. Fiore, Emerging pollutants removal through advanced drinking water treatment: a review on processes and environmental performances assessment, *J. Cleaner Prod.*, 197 (2018) 1210–1221.
- [4] T.R. Sinclair, D. Robles, B. Raza, S. van den Hengel, S.A. Rutjes, A.M. de Roda Husman, J. de Groot, W.M. de Vos, H.D.W. Roesink, Virus reduction through microfiltration membranes modified with a cationic polymer for drinking water applications, *Colloids Surf. A*, 551 (2018) 33–41.
- [5] S. Ebrahim, S. Bou-Hamed, M. Abdel-Jawad, N. Burney, Microfiltration system as a pretreatment for RO units: technical and economic assessment, *Desalination*, 109 (1997) 165–175.
- [6] M.P.O. Gwenaelle, J. Jung, Y. Choi, S. Lee, Effect of microbubbles on microfiltration pretreatment for seawater reverse osmosis membrane, *Desalination*, 403 (2017) 153–160.
- [7] A.F. Corral, U. Yenil, R. Strickle, D. Yan, E. Holler, C. Hill, W.P. Ela, R.G. Arnold, Comparison of slow sand filtration and microfiltration as pretreatments for inland desalination via reverse osmosis, *Desalination*, 334 (2014) 1–9.
- [8] K.-L. Tung, Y.-L. Li, K.-J. Hwang, W.-M. Lu, Analysis and prediction of fouling layer structure in microfiltration, *Desalination*, 234 (2008) 99–106.
- [9] Y. Zhang, Q. Fu, Algal fouling of microfiltration and ultrafiltration membranes and control strategies: a review, *Sep. Purif. Technol.*, 203 (2018) 193–208.
- [10] W. Gao, H. Liang, J. Ma, M. Han, Z.-l. Chen, Z.-s. Han, G.-b. Li, Membrane fouling control in ultrafiltration technology for drinking water production: a review, *Desalination*, 272 (2011) 1–8.
- [11] M. Qasim, N.N. Darwish, S. Mhiyo, N.A. Darwish, N. Hilal, The use of ultrasound to mitigate membrane fouling in desalination and water treatment, *Desalination*, 443 (2018) 143–164.
- [12] K.W. Trzaskus, A. Zdeb, W.M. de Vos, A. Kemperman, K. Nijmeijer, Fouling behavior during microfiltration of silica nanoparticles and polymeric stabilizers, *J. Membr. Sci.*, 505 (2016) 205–215.
- [13] S. Lee, P.-K. Park, J.-H. Kim, K.-M. Yeon, C.-H. Lee, Analysis of filtration characteristics in submerged microfiltration for drinking water treatment, *Water Res.*, 42 (2008) 3109–3121.
- [14] H. Chang, H. Liang, F. Qu, B. Liu, H. Yu, X. Du, G. Li, S.A. Snyder, Hydraulic backwashing for low-pressure membranes in drinking water treatment: a review, *J. Membr. Sci.*, 540 (2017) 362–380.
- [15] L. Li, Z.M. Wang, L.C. Rietveld, N.Y. Gao, J.Y. Hu, D.Q. Yin, S.L. Yu, Comparison of the effects of extracellular and intracellular organic matter extracted from *Microcystis aeruginosa* on ultrafiltration membrane fouling: dynamics and mechanisms, *Environ. Sci. Technol.*, 48 (2014) 14549–14557.
- [16] M. Rahimi, S.S. Madaeni, M. Abolhasani, A.A. Alsairafi, CFD and experimental studies of fouling of a microfiltration membrane, *Chem. Eng. Process. Process Intens.*, 48 (2009) 1405–1413.
- [17] Q.-F. Liu, S.-H. Kim, S. Lee, Prediction of microfiltration membrane fouling using artificial neural network models, *Sep. Purif. Technol.*, 70 (2009) 96–102.
- [18] M. Dalmau, N. Atanasova, S. Gabarrón, I. Rodríguez-Roda, J. Comas, Comparison of a deterministic and a data driven model to describe MBR fouling, *Chem. Eng. J.*, 260 (2015) 300–308.
- [19] K.-J. Hwang, C.-Y. Liao, K.-L. Tung, Analysis of particle fouling during microfiltration by use of blocking models, *J. Membr. Sci.*, 287 (2007) 287–293.
- [20] S. Giglia, G. Straeffler, Combined mechanism fouling model and method for optimization of series microfiltration performance, *J. Membr. Sci.*, 417–418 (2012) 144–153.
- [21] C. Panigrahi, S. Karmakar, M. Mondal, H.N. Mishra, S. De, Modeling of permeate flux decline and permeation of sucrose during microfiltration of sugarcane juice using a hollow-fiber membrane module, *Innov. Food Sci. Emerg. Technol.*, 49 (2018) 92–105.
- [22] M. Tan, G. He, F. Nie, L. Zhang, L. Hu, Optimization of ultrafiltration membrane fabrication using backpropagation neural network and genetic algorithm, *J. Taiwan Inst. Chem. Eng.*, 45 (2014) 68–75.
- [23] H. Shokrkar, A. Salahi, N. Kasiri, T. Mohammadi, Prediction of permeation flux decline during MF of oily wastewater using genetic programming, *Chem. Eng. Res. Design*, 90 (2012) 846–853.

- [24] A.K. Yadav, H. Malik, S.S. Chandel, Selection of most relevant input parameters using WEKA for artificial neural network based solar radiation prediction models, *Renew. Sustain. Energy Rev.*, 31 (2014) 509–519.
- [25] A. Fouladitajar, F. Zokae Ashtiani, A. Okhovat, B. Dabir, Membrane fouling in microfiltration of oil-in-water emulsions; a comparison between constant pressure blocking laws and genetic programming (GP) model, *Desalination*, 329 (2013) 41–49.
- [26] B.I. Hrnjica, GPdotNET V4.0-artificial intelligence tool [Computer program], 2018.
- [27] N. Parveen, S. Zaidi, M. Danish, Support vector regression model for predicting the sorption capacity of lead (II), *Perspect. Sci.*, 8 (2016) 629–631.